The dissipation rate coefficient of turbulence is not universal and depends on the internal stagnation point structure

Susumu Goto[1] and J. C. Vassilicos[2]
[1]*Department of Mechanical Engineering and Science, Kyoto University, Yoshida-Honmachi, Sakyo, Kyoto 606-8501, Japan*
[2]*Department of Aeronautics, Imperial College, London SW7 2AZ, United Kingdom and Institute for Mathematical Sciences, Imperial College, London SW7 2PE, United Kingdom*

(Received 19 September 2008; accepted 19 January 2009; published online 11 March 2009)

The energy dissipation rate coefficient of statistically stationary homogeneous isotropic turbulence depends on the external force sustaining the turbulence irrespective of Reynolds number. This nonuniversality is established by proving that the Taylor length is proportional to the mean distance between stagnation points and thereby relating the energy dissipation rate coefficient to the stagnation point structure of the turbulence which is shown to depend on the structure of the large eddies. Confirmation of these relations is obtained at moderate Reynolds numbers by a series of direct numerical simulations where the large-scale forcing is systematically varied.
 [DOI: 10.1063/1.3085721]

I. THEORY

Taylor stated in 1935 (Ref. 1) that the rate ϵ of turbulent kinetic energy dissipation (per unit mass) is determined by the rms velocity u' and some spatial linear dimension L defining the scale of the system, i.e.,

$$\epsilon = C_\epsilon \frac{u'^3}{L}, \tag{1}$$

where C_ϵ is a constant for high Reynolds number turbulence produced by geometrically similar boundaries. We follow the convention of the past half century,[2] and adopt for L the integral length of the longitudinal velocity correlation function. Since the early 1950s when Batchelor[2] plotted experimental data of C_ϵ in his textbook, the following questions have remained open and at the center of all strands of turbulence research:[3–8] (i) whether C_ϵ is or is not independent of the Reynolds number in the high Reynolds number limit, (ii) whether C_ϵ is or is not independent of the boundary/initial conditions and/or forces which generate the turbulence, and (iii) what determines the value of C_ϵ. These questions are both of fundamental physical importance and engineering turbulence modeling relevance: indeed, C_ϵ is directly related to one of the model parameters of the K-ϵ model, and to the eddy viscosity in large-eddy simulations.

In the present article, by further developing the viewpoint proposed in Ref. 8 and carrying out a series of direct numerical simulations (DNS), we show that C_ϵ is determined by the distribution of *stagnation points* of the turbulent velocity field $\boldsymbol{u}(\boldsymbol{x},t)$. This result suggests that C_ϵ cannot be universal even in the high Reynolds number limit because the stagnation point distribution is determined by the external forcing or boundary conditions irrespective of the Reynolds number. It may be worth mentioning that the fluctuating velocity field $\boldsymbol{u}(\boldsymbol{x},t)$ is Galilean invariant because it is obtained by removing the mean flow from the actual fluid velocity field. Also, stagnation points where $\boldsymbol{u}=(u,v,w)=\boldsymbol{0}$ can be expected to be numerous because they are intersections of the instantaneous line $u(\boldsymbol{x},t)=v(\boldsymbol{x},t)=0$ with the instantaneous surface $w(\boldsymbol{x},t)=0$.

As predicted theoretically[9–11] and confirmed experimentally,[8,12] the mean distance between zero crossings of a component of the turbulent velocity $\boldsymbol{u}$ is proportional to the Taylor length,

$$\lambda = \frac{u'}{\sigma}, \tag{2}$$

where σ is the rms value of the longitudinal velocity derivative. It is important that this property of zero crossings can be generalized (see Appendix A) to the stagnation points of $\boldsymbol{u}$ which are more fluid dynamically meaningful than the zero crossings. More precisely, as we show in Appendix A under relatively weak assumptions, the number density n_s per unit volume of the stagnation points of $\boldsymbol{u}$ is related to λ by

$$\lambda = B n_s^{-1/3}, \tag{3}$$

where B is a constant (unless the Reynolds number is too small or small-scale intermittency effects are taken into account in which case B may be a very weak function of the Reynolds number; see Appendix A).

On the other hand, it has been shown[13,14] that the number density $n_s^{(c)}$ of stagnation points in the coarse-grained velocity field $\boldsymbol{u}^{(c)}$ at the cutoff length scale ℓ_c obeys the following formula:

$$n_s^{(c)}(\ell_c) = \begin{cases} C_s \dfrac{1}{L_*^3}\left(\dfrac{L_*}{\ell_c}\right)^{D_s} & \text{for} \quad \eta \ll \ell_c \ll L, \\ C_s \dfrac{1}{L_*^3}\left(\dfrac{L_*}{\eta}\right)^{D_s} \quad (=n_s) & \text{for} \quad \ell_c \ll \eta. \end{cases} \tag{4}$$

Note that, in practice, the coarse-grained velocity field $\boldsymbol{u}^{(c)}$ and therefore $n_s^{(c)}$ do not depend appreciably on the type of low-pass filter if it is sufficiently high order.[8] Here, the inner cutoff η is proportional to the Kolmogorov length η_K, i.e.,

$$\eta = A\,\eta_K = A(\nu^3/\epsilon)^{1/4} \tag{5}$$

(A and ν being a dimensionless constant and the kinematic viscosity of the fluid, respectively) and L_* is a reference length such that $\eta \lesssim L_* \lesssim L$. In our previous studies, we set $L_*=L$ for simplicity, but the introduction of the reference length L_* is essential for Sec. III where we set $\ell_c=L_*$ in order to numerically estimate C_s, a procedure which is not possible without the introduction of a reference length L_* smaller than L. In Eq. (4), C_s and D_s are constants, and D_s is related to the exponent p of the energy spectrum $E(k)\sim k^{-p}$ (in the range $\eta \ll k^{-1} \ll L$) of the velocity field $\boldsymbol{u}$ by

$$D_s = \frac{3(3-p)}{2}. \tag{6}$$

A simple schematic derivation of the fractal dimension (6) is given in Appendix B. Note that the inner cutoff η of scaling (4) may not actually be proportional to the Kolmogorov length as shown experimentally in Ref. 8 for zero crossings where A in Eq. (5) turned out to be an increasing function of $\log R_\lambda$. However, for simplicity, we do not take into account this small correction here and assume A to be independent of Reynolds number. We return to this point in the last section.

From $\epsilon = 15\nu u'^2/\lambda^2$ in conjunction with Eqs. (3)–(5) we obtain

$$\epsilon = [15u'^2 A^{-2D_s/3} B^{-2} C_s^{2/3} L_*^{-2+2D_s/3} \nu^{1-D_s/2}]^{1/(1-D_s/6)}. \tag{7}$$

Then, using the Reynolds number independence of A and B as $\nu \to 0$ (or, more generally, assuming the Reynolds number independence of $BA^{D_s/3}$ as $\nu \to 0$), it follows that the energy dissipation ϵ is independent of ν in that limit provided that $D_s=2$ which corresponds to

$$p = \tfrac{5}{3} \tag{8}$$

in Eq. (6). The Taylor relation (1) then follows with the coefficient

$$C_\epsilon = \frac{15^{3/2} C_s}{A^2 B^3} \frac{L}{L_*}. \tag{9}$$

Note that Eq. (8) corresponds to the well-known $-5/3$ power law spectrum[15] which we have derived here using the generalized Rice theorem (Appendix A). Since we have made the same assumption about ϵ as was made by Kolmogorov in the high Reynolds number limit,[15] it may not be too surprising that we reach the same conclusion on the energy spectrum. However, it is not trivial that the dissipation coefficient C_ϵ is related to a constant C_s which characterizes the large-scale spatial distribution of stagnation points and therefore one basic aspect of large-scale flow topology. It may be worth noting that this relation (9) can also be derived without any assumptions on the Reynolds number dependencies of A and B if use is made of $D_s=2$ on account of $p=5/3$ and Eq. (6). In this case, both sides of Eq. (9) are Reynolds number dependent, in principle, as is undoubtedly the case when the Reynolds number is not large enough. In Sec. III we provide DNS support for Eq. (9) at Reynolds numbers where both sides of Eq. (9) are Reynolds number dependent.

Note that the reference length L_* in Eq. (4) is arbitrary as long as it lies in the scaling range $\eta \lesssim L_* \lesssim L$. However, our conclusions do not depend on the choice of L_*. Although the reference length L_* appears on the right-hand side of Eq. (9), C_ϵ does not depend on L_* because C_s also depends on the choice of L_*. If we choose another reference length, say $\tilde{L}_*$, the coefficient in Eq. (4) is $\tilde{C}_s = \tilde{L}_*^3 n_s^{(c)}(\ell_c=\tilde{L}_*)$ which equals $C_s(\tilde{L}_*/L_*)^{3-D_s}$. Then, setting $D_s=2$ for Eq. (9) to hold, both choices of L_* lead to the same dissipation coefficient C_ϵ.

An important consequence of Eq. (9) is that the coefficient C_ϵ in the Taylor relation (1) may not be universal. This is because C_s is the number of stagnation points in a cube of side L_* in the coarse-grained velocity field at the reference scale L_*, i.e., $L_*^3 n_s^{(c)}(L_*)$, and because it depends on the large-scale structures. Note that L_* can be as large as the integral length. This conclusion may seem to be in conflict with a recent report[5] based on the currently highest Reynolds number DNS available, but this is not so because these DNS were carried out with a common large-scale structure. The nonuniversality of C_ϵ has already been reported from comparisons of DNS with different external forcings (although with limited Reynolds numbers) (Ref. 4) and from analyses of experimental data (see Refs. 3 and 8 and references therein).

The purpose of what follows is to demonstrate the nonuniversality of C_ϵ and of $(C_s L)/(B^3 L_*)$, but also the proportionality between them, by a systematic series of DNS with different large-scale structures.

II. DIRECT NUMERICAL SIMULATIONS

Statistically homogeneous isotropic turbulence is simulated by numerically integrating the Navier–Stokes equations for an incompressible fluid in a periodic box (with period 2π) using the fourth-order Runge–Kutta method. Spatial derivatives in the equations are estimated by a dealiased Fourier spectral method. We report results based on the analysis of such turbulence simulated using 1024^3 grid points.

The initial condition of each DNS is taken from a lower resolution (512^3) velocity field in statistically stationary state. This lower resolution field has been obtained from a DNS with an initially random velocity field with prescribed spectrum

$$E(k) = \begin{cases} C_E k^q \exp\left[-\dfrac{q}{2}\left(\dfrac{k}{k_0}\right)^2\right] & \text{for} \quad k \le k_0, \\ C_E k^q \exp\left[-\dfrac{q}{\alpha}\left(\dfrac{k}{k_0}\right)^\alpha + \dfrac{q}{\alpha} - \dfrac{q}{2}\right] & \text{for} \quad k_0 \le k. \end{cases} \tag{10}$$

Here, the coefficient C_E is chosen such that the total kinetic energy in the 512^3 simulation is unity; the exponent q in the small wavenumber range is either 2 or 4; the wavenumber k_0 where the energy spectrum peaks is either 5, 10, or 15; and the other exponent α in the exponential function is chosen ($\alpha=1$ for $q=2$, and 1/2 for 4) such that the energy spectrum of the 1024^3 simulation is a smooth function at the border wavenumber (k_f, see below) between forced and unforced wavenumber ranges. We have carried out 24 different runs for 24 different combinations of the large-scale structure

TABLE I. Numerical parameters of the DNS, and statistics (time-averaged values in the statistically stationary state) of simulated turbulence. Note that the index $k_{\max}\eta_K$, where $k_{\max}=(\sqrt{2}/3)\times 1024\approx 482$ is the largest wavenumber of the DNS dealiased by the phase shift method, is smaller than 1 in some of our simulations. This suggests that the smallest scale motions might not be fully well resolved in those simulations with small ν. However, the dependence of C_ϵ on R_λ appears smooth in Fig. 3 suggesting that our values of $k_{\max}\eta_K$ are suitable for this paper's purposes which are concerned with C_ϵ.

q	k_0	ν ($\times 10^{-4}$)	R_λ	L	λ ($\times 10^{-2}$)	η_K ($\times 10^{-3}$)	u'	ϵ	T	$k_{\max}\eta_K$
2	5	6.250	117	0.313	7.35	3.45	0.995	1.71	0.314	1.66
2	5	5.000	131	0.311	6.60	2.92	0.996	1.70	0.312	1.40
2	5	3.750	152	0.310	5.75	2.36	0.995	1.68	0.311	1.13
2	5	3.125	168	0.308	5.27	2.06	0.996	1.67	0.309	0.99
2	10	6.250	81.7	0.165	5.27	2.96	0.969	3.16	0.171	1.42
2	10	5.000	91.9	0.162	4.69	2.48	0.979	3.27	0.165	1.19
2	10	3.750	107	0.159	4.04	1.99	0.988	3.35	0.161	0.95
2	10	3.125	117	0.158	3.70	1.73	0.991	3.36	0.159	0.83
2	15	6.250	65.2	0.116	4.34	2.73	0.938	4.36	0.124	1.31
2	15	5.000	73.8	0.113	3.86	2.28	0.956	4.60	0.118	1.09
2	15	3.750	86.3	0.109	3.32	1.81	0.974	4.83	0.112	0.87
2	15	3.125	95.1	0.107	3.02	1.57	0.981	4.92	0.109	0.75
4	5	6.250	110	0.267	7.11	3.44	0.969	1.74	0.275	1.65
4	5	5.000	123	0.265	6.37	2.91	0.971	1.74	0.273	1.40
4	5	3.750	144	0.263	5.56	2.35	0.972	1.71	0.270	1.13
4	5	3.125	158	0.263	5.10	2.05	0.971	1.69	0.271	0.99
4	10	6.250	76.5	0.141	5.06	2.94	0.944	3.26	0.149	1.41
4	10	5.000	86.2	0.138	4.50	2.46	0.956	3.37	0.144	1.18
4	10	3.750	100	0.135	3.89	1.97	0.965	3.45	0.140	0.95
4	10	3.125	110	0.133	3.55	1.72	0.968	3.47	0.138	0.82
4	15	6.250	60.7	0.0992	4.15	2.70	0.913	4.53	0.108	1.30
4	15	5.000	69.0	0.0961	3.69	2.26	0.932	4.76	0.103	1.08
4	15	3.750	80.8	0.0929	3.18	1.79	0.951	5.02	0.0976	0.86
4	15	3.125	89.2	0.0914	2.90	1.56	0.959	5.12	0.0952	0.75

(q,k_0) and the kinematic viscosity ν. Numerical parameters adopted in our DNS are given in the first three columns of Table I.

The external large-scale forcing is implemented numerically by keeping the magnitudes of the Fourier components of velocity fixed in the low wavenumber range $k<k_f=2.4k_0$. The value 2.4 has been chosen for the energy spectrum to be as smooth as possible at k_f. Note, however, that the phases of these Fourier components evolve temporally, and that the large-scale velocity field is therefore not steady.

After several large-eddy turnover times $T=L/u'$, turbulence reaches a statistically stationary state. The temporal averages of the Reynolds number

$$R_\lambda = \frac{\lambda u'}{\nu} \tag{11}$$

and the Taylor length $\lambda=\sqrt{15\nu u'^2/\epsilon}$ in this state are shown in Table I together with the temporal averages of the integral length L, the Kolmogorov length η_K, the rms velocity u', the energy dissipation rate ϵ and the large-eddy turnover time T. Here, we estimate the integral length L by integrating the energy spectrum $E(k)$ as follows:

$$L = \frac{3\pi}{4}\int_0^\infty E(k)k^{-1}dk \Big/ \int_0^\infty E(k)dk. \tag{12}$$

As seen in Fig. 1, $E(k)$ exhibits two power laws in the statistically stationary state: $E(k)\sim k^q$ for $k\ll k_0$ and $E(k)\sim k^{-5/3}$ for $k_0\ll k$ ($\ll 2\pi/\eta_K$). We plot eight curves, in each figure of Fig. 1, which correspond to different combinations of the exponents q and the kinematic viscosities ν. For the same q, the behavior of $E(k)$ in the energy containing range is identical for different values of ν, whereas for the same ν, the behavior in the dissipation range seems almost identical for different values of q in these logarithmic plots.

III. VERIFICATION OF EQ. (9)

We plot in Fig. 2 the temporal evolution of the dissipation coefficient C_ϵ for each simulation where $\nu=6\times 10^{-4}$. (Other ν cases have similar behaviors.) Here, ϵ is estimated from $\epsilon=\nu Q$ where Q is the enstrophy. Probably because we fix the energy spectrum at the lower wavenumbers, there are only very small temporal fluctuations on this coefficient in the statistically stationary state. These temporal fluctuations, if at all perceptible, are negligible compared to the very significant differences in C_ϵ which result from different large-

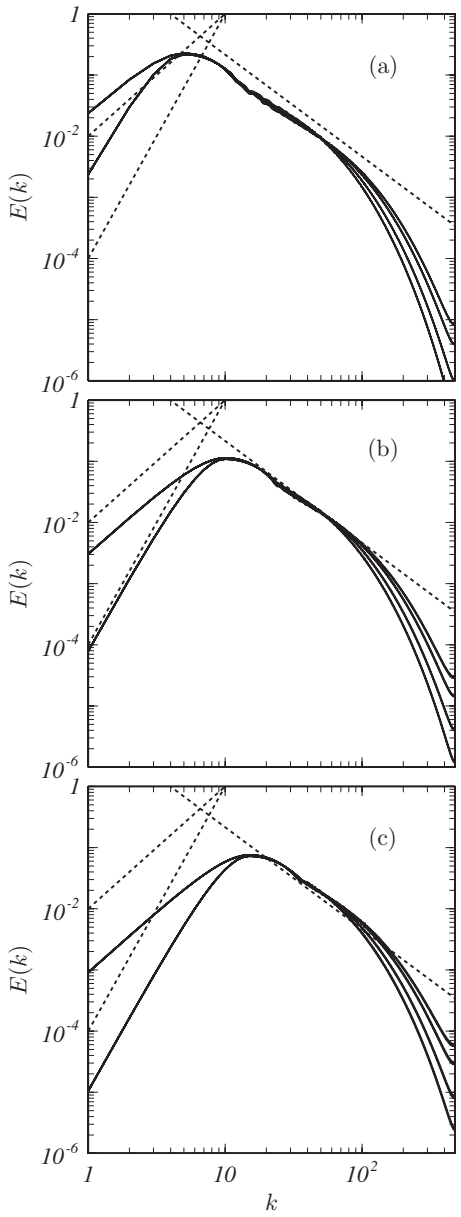

FIG. 1. Energy spectra at the final time of each simulation for the three different peak wavenumbers: (a) $k_0=5$, (b) 10, and (c) 15. In each figure, we plot eight curves for all combinations of the four different kinematic viscosities and the two different low wavenumber exponents ($q=2$ or 4) of the energy spectrum [$E(k)\sim k^q$ for $k\ll k_0$]. The dotted lines indicate power laws with exponents $-5/3$, 2, and 4.

scale parameters. These differences are clear and unambiguous throughout the time of our simulations, and it therefore makes sense, as we do in Fig. 3(a), to plot the value of C_ϵ at the final instant of each simulation as a function of Reynolds number R_λ. It is clearly observed that the coefficient C_ϵ depends not only on the Reynolds number R_λ but also on the exponent q of the energy spectrum $E(k)\sim k^q$ in the low wavenumber range $k\ll k_0$. The fact that, for different values of q, there are distinct $C_\epsilon(R_\lambda)$ curves which appear to asymptote toward different constants as the Reynolds number increases supports the view that C_ϵ is not universal and depends on the large-scale structure even asymptotically $(R_\lambda\to\infty)$.

In order to verify Eq. (9), we need to estimate C_s/B^3.

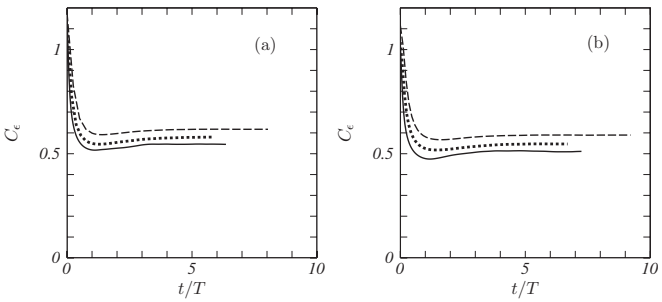

FIG. 2. Temporal evolution of the dissipation coefficient C_ϵ. (a) $(q,\nu)=(2,6.25\times10^{-4})$, (b) $(q,\nu)=(4,6.25\times10^{-4})$. Solid curves, $k_0=5$; dotted curves, $k_0=10$; dashed curves, $k_0=15$.

However, since our simulations possess only limited inertial ranges, it is hard to estimate the coefficient C_s in Eq. (4) by fitting data for $n_s^{(c)}$ with the scaling form (4). Instead, we estimate C_s by the relation

$$C_s = L_*^3 n_s^{(c)}(\ell_c = L_*). \tag{13}$$

The number density of the stagnation points in the coarse-grained field at the length scale L_* may be counted numerically, but the number of such points is not large enough if we choose L_* too close to L. We therefore use an alternative estimation of $n_s^{(c)}$ which proceeds by introducing the coarse-grained field's Taylor scale

$$\lambda^{(c)} = \sqrt{5\int_0^{2\pi/L_*} E(k)dk \Big/ \int_0^{2\pi/L_*} k^2 E(k)dk}. \tag{14}$$

The number density $n_s^{(c)}$ is then obtained by application of the generalized Rice theorem to the coarse-grained field which gives

$$n_s^{(c)} = \left(\frac{B}{\lambda^{(c)}}\right)^3. \tag{15}$$

From Eqs. (13) and (15) we obtain

$$\frac{C_s}{B^3} = \left(\frac{L_*}{\lambda^{(c)}}\right)^3, \tag{16}$$

which we use to estimate C_s/B^3 from our simulations.

Because of the assumptions under which the generalized Rice theorem is derived (see Appendix A), B in Eqs. (15) and (16) may be considered constant if L/L_* and R_λ are large enough. In our DNS, however, R_λ is not so large and B can therefore be expected to have a residual dependence on it. This is confirmed in Fig. 3(b) where we plot C_s/B^3 as a function of R_λ. In this plot, C_s/B^3 is estimated from (16) by choosing $L_*=0.2L$ so as to make sure that L_* is within the inertial range, and that L/L_* is as large as possible in our DNS.

One of the interesting observations in Figs. 3(a) and 3(b) is that both C_ϵ [Fig. 3(a)] and C_s/B^3 [Fig. 3(b)] are clearly dependent on R_λ and q. We use Eq. (9) to define the normalized dissipation coefficient

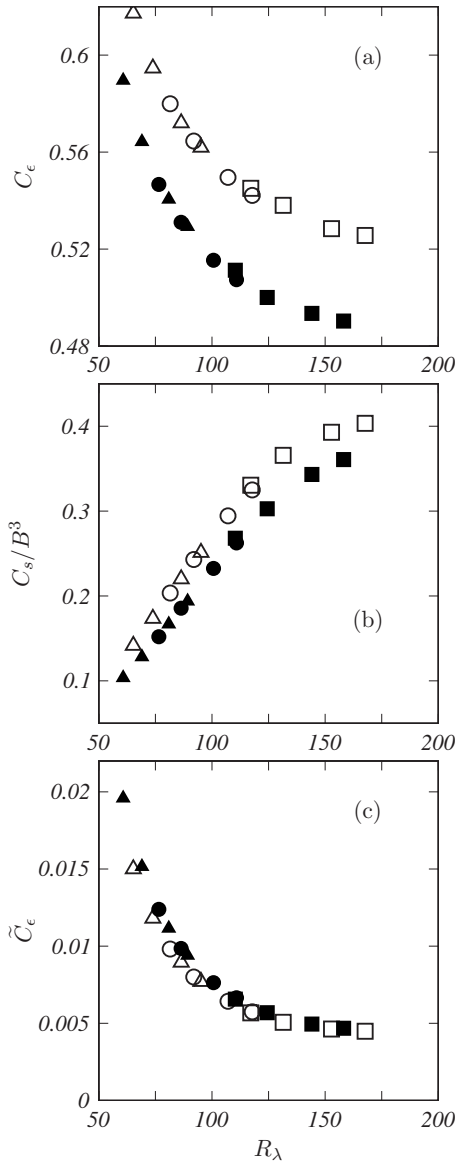

FIG. 3. Plots as functions of R_λ of (a) the energy dissipation coefficient C_ϵ; (b) the stagnation point coefficient C_s/B^3; (c) and the normalized dissipation coefficient. Open symbols, $q=2$; solid symbols, $q=4$. Squares, $k_0=5$; circles, $k_0=10$; triangles, $k_0=15$.

$$\tilde{C}_\epsilon = \frac{C_\epsilon}{(15^{3/2}C_s L)/(B^3 L_*)} \quad \left(=\frac{1}{A^2}\right), \tag{17}$$

which we plot in Fig. 3(c) as a function of R_λ. This plot clearly shows that C_ϵ and C_s/B^3 have the same dependence on the large-scale structure (i.e., q) even at low R_λ, and it strongly supports the validity of Eq. (9) because A depends only on R_λ. The plot seems also to suggest that $\tilde{C}_\epsilon$ tends to a constant with increasing R_λ, thus implying that the dependence of C_ϵ on the large-scale structures and the independence of $\tilde{C}_\epsilon$ on these structures survive even in the limit $R_\lambda \to \infty$.

However, it is not conclusive from Fig. 3(a) whether, for a fixed q, C_ϵ does or does not become a constant in the limit $R_\lambda \to \infty$. Also, we are unable to determine A independently and directly from Eq. (4) with the kind of accuracy which would allow to fully validate Eq. (9) quantitatively. Nevertheless, Fig. 3(c) suggests that $A \approx 10$ at high R_λ, which is consistent with the experimental data[8] on zero crossings, and with the well-known fact that the inertial range of the energy spectrum is bounded by about one tenth of the Kolmogorov wavenumber. Figure 3 also suggests that much, although not all, of the Reynolds number dependence of C_ϵ is accountable to the Reynolds number dependence of A, in agreement with the conclusions in Ref. 8.

Incidentally, the coefficient B can be expected to have a residual dependence on L_* if L_* is not small enough. We have checked that the coincidence observed in Fig. 3(c) is preserved even if we adopt a different L_*, although the absolute value of $\tilde{C}_\epsilon$ depends on its choice particularly if L_* is not small enough because of the residual dependence of B on L_*.

As a final point, we use Eq. (16) to show that Eq. (9) can yield the relation (22) between C_ϵ and q which is similar to the one recently derived and used in Ref. 7. If we assume that $E(k)$ has the high R_λ model functional form

$$E(k) = \begin{cases} C_E k^q & \text{for} \quad k \le k_0, \\ C_E k_0^{q+5/3} k^{-5/3} & \text{for} \quad k_0 \le k, \end{cases} \tag{18}$$

the integral length (12) becomes

$$L = \frac{3\pi}{4} \frac{\frac{1}{q} + \frac{3}{5}}{\frac{1}{q+1} + \frac{3}{2}} k_0^{-1}. \tag{19}$$

Defining $k_* = 2\pi/L_*$ and assuming it to be in the inertial range (i.e., $k_* \gg k_0$), the Taylor scale $\lambda^{(c)}$ defined by Eq. (14) takes the form

$$\lambda^{(c)} = \sqrt{\frac{10(3q+5)}{3(q+1)}} k_0^{-1/3} k_*^{-2/3}. \tag{20}$$

Therefore, from Eq. (16), we obtain

$$C_s = (2\pi B)^3 \left[\frac{3(q+1)}{10(3q+5)}\right]^{3/2} \frac{k_0}{k_*}. \tag{21}$$

Then, Eq. (9) leads to

$$C_\epsilon = \frac{3\pi^3}{A^2} \left[\frac{9(q+1)}{2(3q+5)}\right]^{3/2} \frac{\frac{1}{q} + \frac{3}{5}}{\frac{1}{q+1} + \frac{3}{2}}, \tag{22}$$

which implies that C_ϵ depends on q, the exponent of $E(k)$ in the low wavenumber range, even in the high Reynolds number limit (i.e., $L/\eta \to \infty$). Note that C_ϵ in Eq. (22) depends only on q (but is independent of k_0), and is a decreasing function of q. These points are consistent with Fig. 3(a). Furthermore, the ratio $C_\epsilon(q=2)/C_\epsilon(q=4)$ predicted by Eq. (22) is about 1.071, which is almost identical to the ratio $0.525/0.490 \approx 1.071$ at the highest Reynolds number of our DNS plotted in Fig. 3.

IV. CONCLUSION

By considering the statistics of the spatial distribution of stagnation points, we can suggest answers to two (ii and iii) of the three open questions mentioned in the first section. That is, the dissipation coefficient C_ϵ is not universal, and it depends on the internal stagnation point structure of the turbulence, which itself depends on the structure of the large eddies.

However, we have not answered the question (i) whether C_ϵ is asymptotically independent of the Reynolds number. Instead we have shown that if we assume it is, we can then use the generalized Rice theorem and Eq. (4) to derive the Kolmogorov wavenumber form of the energy spectrum and relation (9) between C_ϵ and C_s/B^3. Incidentally, this relation (9) can also be obtained without an assumption on the Reynolds number dependence of C_ϵ: assuming a Kolmogorov shaped energy spectrum, i.e., $p=5/3$, and using Eq. (6) to derive $D_s=2$ also leads to Eq. (9). As observed in Fig. 3(a), for a common large-scale structure, C_ϵ is a monotonically decreasing function of R_λ, but the dependence seems to be weaker for higher R_λ in this linear-linear plot. In order to determine the subtle asymptotic R_λ dependence or independence of C_ϵ, we must carefully consider small-scale intermittency effects and the resulting R_λ dependence of the constant B in the generalized Rice theorem (3) (see Appendix A) as well as the R_λ dependence of A, the ratio of the inner cutoff length to the Kolmogorov length [recall the statements below Eq. (6)]. However, as experimentally suggested[8] for zero crossings, these dependencies on R_λ may be logarithmic and the verification of such weak dependencies is beyond the scope of the present paper which is based on DNS carried out over a narrow R_λ range.

Another important work which must be left for future much larger DNS is the extension of this paper's arguments to decaying turbulence so as to shed some light on the so-called permanence of large eddies. This seems a natural direction to follow because the spatial distribution of stagnation points in the turbulence is determined by the large-scale eddies and because the permanence of large eddies is therefore likely to be related to the permanence of a statistical property of stagnation points.

ACKNOWLEDGMENTS

The DNS were carried out on NEC SX-7/160M5 with the support of the NIFS Collaborative Program.

APPENDIX A: THE GENERALIZED RICE THEOREM

The generalized Rice theorem states that, for large enough Reynolds number, the average distance between stagnation points of an incompressible statistically isotropic and homogeneous turbulent velocity field is proportional to the field's Taylor scale provided that the velocity field and its spatial derivatives are statistically independent and provided that the shapes of the probability density functions (PDF) of the velocity components on the one hand and the velocity derivatives on the other are independent of Reynolds number and can be scaled, respectively, with u' and $\sigma=\langle u_x^2\rangle^{1/2}$. Here $u_x=\partial u/\partial x$. It is also required that the PDF of velocity derivatives decays fast enough at infinity. The generalization is twofold: The assumptions have been relaxed, and the statement is about stagnation points rather than zero crossings. We now prove this statement.

The number N_s of stagnation points $\boldsymbol{u}=(u,v,w)=\mathbf{0}$ in a given volume can be expressed as an integral over that volume:

$$N_s=\int dV|\nabla H[u(\boldsymbol{x})]||\nabla H[v(\boldsymbol{x})]||\nabla H[w(\boldsymbol{x})]|, \tag{A1}$$

where H is the Heaviside function. This formula leads to

$$N_s=\int dV\delta[(u(\boldsymbol{x})\ ]\delta[(v(\boldsymbol{x})\ ]\delta[(w(\boldsymbol{x})\ ]|\nabla u||\nabla v||\nabla w|, \tag{A2}$$

where δ is the delta function. Statistical homogeneity allows us to replace this volume integral by an average weighted by the joint PDF $P(\boldsymbol{u},\nabla\boldsymbol{u})$. We therefore obtain the following expression for the number density n_s per unit volume

$$n_s=\int d\boldsymbol{u}du_xdu_ydu_zdv_xdv_ydv_zdw_xdw_ydw_z\delta(u)\delta(v)\delta(w)P(\boldsymbol{u},\nabla\boldsymbol{u})\sqrt{u_x^2+u_y^2+u_z^2}\sqrt{v_x^2+v_y^2+v_z^2}\sqrt{w_x^2+w_y^2+w_z^2}, \tag{A3}$$

$$=\int du_xdu_ydu_zdv_xdv_ydv_zdw_xdw_ydw_zP(\boldsymbol{u}=\mathbf{0},\nabla\boldsymbol{u})\sqrt{u_x^2+u_y^2+u_z^2}\sqrt{v_x^2+v_y^2+v_z^2}\sqrt{w_x^2+w_y^2+w_z^2}. \tag{A4}$$

Following Rice[9–11] we assume statistical independence between $\boldsymbol{u}$ and $\nabla\boldsymbol{u}$, specifically $P(\boldsymbol{u}=\mathbf{0},\nabla\boldsymbol{u})=P_l(\boldsymbol{u}=\mathbf{0})P_s(\nabla\boldsymbol{u})$ (where the suffixes l and s stand for large scale and small scale, respectively), which leads to

$$n_s=P_l(\boldsymbol{u}=\mathbf{0})\int du_xdu_ydu_zdv_xdv_ydv_zdw_xdw_ydw_zP_s(\nabla\boldsymbol{u})\sqrt{u_x^2+u_y^2+u_z^2}\sqrt{v_x^2+v_y^2+v_z^2}\sqrt{w_x^2+w_y^2+w_z^2}. \tag{A5}$$

At this stage we assume statistical isotropy but we need to do this within the constraints of incompressibility. As demonstrated by Taylor,[1] a statistically isotropic velocity gradient tensor field resulting from an incompressible velocity field obeys the following relations between averages of velocity gradient products: $\langle u_xv_y\rangle=\langle v_yw_z\rangle=\langle w_zu_x\rangle=\langle u_yv_x\rangle=\langle u_zw_x\rangle=\langle w_yv_z\rangle=-\frac{1}{2}\langle u_x^2\rangle=-\frac{1}{2}\langle v_y^2\rangle=-\frac{1}{2}\langle w_z^2\rangle$, $2\langle u_x^2\rangle=\langle u_y^2\rangle=\langle u_z^2\rangle$, $2\langle v_y^2\rangle=\langle v_x^2\rangle=\langle v_z^2\rangle$, $2\langle w_z^2\rangle=\langle w_x^2\rangle=\langle w_y^2\rangle$, and the averages of all other products of

two velocity gradients vanish. These relations are satisfied if we make the assumption that the nondimensional form of the PDF P_s can be written in terms of the single strain rate $\sigma=\langle u_x^2\rangle^{1/2}$. Specifically,

$$P_s(\nabla \boldsymbol{u})du_x du_y du_z dv_x dv_y dv_z dw_x dw_y dw_z = P_s(\nabla \boldsymbol{u}/\sigma)d\left(\frac{u_x}{\sigma}\right)d\left(\frac{u_y}{\sigma}\right)d\left(\frac{u_z}{\sigma}\right)d\left(\frac{v_x}{\sigma}\right)d\left(\frac{v_y}{\sigma}\right)d\left(\frac{v_z}{\sigma}\right)d\left(\frac{w_x}{\sigma}\right)d\left(\frac{w_y}{\sigma}\right)d\left(\frac{w_z}{\sigma}\right). \tag{A6}$$

This assumption replaces and is more general than Rice's assumption of Gaussianity of velocity derivatives. A similar assumption can be made for $P_l(\boldsymbol{u})$ which was also assumed by Rice to be Gaussian. Here we only assume $P_l(\boldsymbol{u})d\boldsymbol{u} = P_l(\boldsymbol{u}/u')d\boldsymbol{u}/u'^3$ in agreement with our assumption of isotropy which demands that $u'^2=\langle u^2\rangle=\langle v^2\rangle=\langle w^2\rangle$. Clearly, appropriate Gaussian forms for the large-scale and small-scale distributions are particular cases which satisfy our scaling assumptions on P_s and P_l.

It follows that $P_l(\boldsymbol{u}/u'=\boldsymbol{0})\sim u'^{-3}$ and therefore that

$$n_s \sim u'^{-3}\sigma^3. \tag{A7}$$

Hence,

$$n_s^{-1/3} = B\frac{u'}{\sigma} = B\lambda, \tag{A8}$$

where B is a dimensionless constant determined by the actual value of $P_l(\boldsymbol{u}/u'=\boldsymbol{0})$ and by the details of the probability distribution P_s. If we finally assume this value and this distribution to be independent of Reynolds number, then the generalized Rice theorem is established as it then follows that B is also independent of Reynolds number. [The benign assumption that the PDF of velocity derivatives decays fast enough at infinity ensures that the integral in Eq. (A5), and therefore B, are finite.]

While it is reasonable to expect that $P_l(\boldsymbol{u}=\boldsymbol{0})$ is independent of Reynolds number, it is well known that the PDF of turbulence velocity derivatives become increasingly non-Gaussian with increasing Reynolds number because of small-scale intermittency. There may therefore be a resulting dependence of B on Reynolds number, but the results on zero crossings presented in Ref. 8 suggest that this dependence might be as weak as logarithmic. If the Reynolds number is too small, then the PDF of turbulence velocity derivatives can have a residual Reynolds number dependence caused by insufficient development of inertial range dynamics. Our assumption is that the Reynolds number is large enough for this not to happen and that small-scale intermittency effects are negligible in this limit, so that B is asymptotically independent of the Reynolds number as a result.

In pages 26 to 29 of a recent book by Joseph *et al.*[16] a relation is found between dissipation and number of stagnation points in a Taylor vortex array. This relation corresponds to a Rice theorem and a relation such as Eq. (9) for the particular flow considered by these authors.

APPENDIX B: A SIMPLE SCHEMATIC DERIVATION OF EQ. (6)

We estimate the fractal dimension D_s of the set of velocity stagnation points of a velocity field where the energy spectrum $E(k)$ obeys

$$E(k) \sim k^{-p} \tag{B1}$$

in the scaling range,

$$\frac{1}{L} \ll k \ll \frac{1}{\eta}. \tag{B2}$$

Note that the second-order structure function of the x-components of the velocity has the scaling

$$\langle |u(x+r)-u(x)|^2\rangle \sim r^{p-1}. \tag{B3}$$

First, let D be the fractal dimension of the surface where the component $u=0$. Assuming isotropy, the surface where $v=0$ and the surface where $w=0$ have the same dimension D. The formula of codimensions for intersections of surfaces yields

$$D_s = 3(D-2) \tag{B4}$$

because all three components of the velocity vector vanish at a stagnation point.

Second, the dimension D_1 of the graph of $u(x)$ is

$$D_1 = D-1. \tag{B5}$$

[This is also derived by the formula of the codimensions. That is, the dimension of the zero crossings of $u(x)$ is $3-((3-D)+(3-1))=D-2$. Therefore, from $(2-D_1)+(2-1)=2-(D-2)$, we obtain Eq. (B5).] This means that the length $\ell(r)$ of the graph at a scale r is, by definition of the fractal dimension,

$$\ell(r) \sim r^{1-D_1} = r^{2-D}. \tag{B6}$$

The length $\ell(r)$ can also be estimated as

$$\ell(r) \sim r^{-1}\sqrt{r^2+\langle |u(x+r)-u(x)|^2\rangle} \tag{B7}$$

if we assume that every part of the graph within a segment of size r along the x-axis is statistically similar to all the others and use the fact that the number of these segments is proportional to r^{-1}. Using Eq. (B3), Eq. (B7) reduces to

$$\ell(r) \sim r^{-1+(p-1)/2} = r^{(p-3)/2}. \tag{B8}$$

Then, the comparison of the exponents of Eqs. (B6) and (B8) leads to

$$D = \frac{7-p}{2}. \tag{B9}$$

Orey[14] proved this relation Eq. (B9) rigorously for Gaussian stochastic functions.

Substituting Eq. (B9) into Eq. (B4), we arrive at Eq. (6).

[1] G. I. Taylor, "Statistical theory of turbulence," Proc. R. Soc. London, Ser. A **151**, 421 (1935).

[2] G. K. Batchelor, *The Theory of Homogeneous Turbulence* (Cambridge University Press, Cambridge, England, 1953).

[3] K. R. Sreenivasan, "On the scaling of the turbulence energy dissipation rate," Phys. Fluids **27**, 1048 (1984).

[4] K. R. Sreenivasan, "An update on the energy dissipation rate in isotropic turbulence," Phys. Fluids **10**, 528 (1998).

[5] Y. Kaneda, T. Ishihara, M. Yokokawa, K. Itakura, and A. Uno, "Energy dissipation rate and energy spectrum in high resolution direct numerical simulations of turbulence in a periodic box," Phys. Fluids **15**, L21 (2003).

[6] P. Burattini, P. Lavoie, and R. A. Antonia, "On the normalized turbulent energy dissipation rate," Phys. Fluids **17**, 098103 (2005).

[7] W. J. T. Bos, L. Shao, and J.-P. Bertoglio, "Spectral imbalance and the normalized dissipation rate of turbulence," Phys. Fluids **19**, 045101 (2007).

[8] N. Mazellier and J. C. Vassilicos, "The turbulence dissipation constant is not universal because of its universal dependence on large-scale flow topology," Phys. Fluids **20**, 015101 (2008).

[9] S. O. Rice, "Mathematical analysis of random noise," Bell Syst. Tech. J. **23**, 282 (1944).

[10] S. O. Rice, "Mathematical analysis of random noise," Bell Syst. Tech. J. **24**, 46 (1945).

[11] H. W. Liepmann and M. S. Robinson, "Counting methods and equipment for mean-value measurements in turbulence research," Washington, Report No. NACA TN 3037, 1953.

[12] K. R. Sreenivasan, A. Prabhu, and R. Narasimha, "Zero-crossing in turbulent signals," J. Fluid Mech. **137**, 251 (1983).

[13] J. Dávila and J. C. Vassilicos, "Richardson's pair diffusion and the stagnation point structure of turbulence," Phys. Rev. Lett. **91**, 144501 (2003).

[14] S. Orey, "Gaussian sample functions and the Hausdorff dimension of level crossing," Z. Wahrscheinlichkeitstheor. Verwandte Geb. **15**, 249 (1970).

[15] U. Frisch, *Turbulence: The Legacy of A. N. Kolmogorov* (Cambridge University Press, Cambridge, England, 1995).

[16] D. Joseph, T. Funada, and J. Wang, *Potential Flows of Viscous and Viscoelastic Fluids* (Cambridge University Press, Cambridge, England, 2008).